Title

Characterization of long period return values of extreme daily temperature and precipitation in the CMIP6 models: Part 2, projections of future change

Author

Wehner, Michael F

Publication Date

2020-12-01

DOI

10.1016/j.wace.2020.100284

Peer reviewed

Weather and Climate Extremes 30 (2020) 100284

Contents lists available at ScienceDirect

Weather and Climate Extremes

journal homepage: http://www.elsevier.com/locate/wace

Characterization of long period return values of extreme daily temperature and precipitation in the CMIP6 models: Part 2, projections of future change

Michael F. Wehner

Lawrence Berkeley National Laboratory, Berkeley, CA, USA

A B S T R A C T

Using a non-stationary Generalized Extreme Value statistical method, projected future changes in selected extreme daily temperature and precipitation indices and their 20 year return values from the CMIP5 and CMIP6 climate models are calculated and compared. Projections are framed in terms of specified global warming target temperatures rather than at specific times and under specific emissions scenarios. The change in framing shifts projection uncertainty due to differences in model climate sensitivity from the values of the projections to the timing of the global warming target. At their standard resolutions, there are no meaningful differences between the two generations of models in their projections of simulated extreme daily temperature and precipitation at specified global warming targets.

1. Introduction

The projection of future changes in extreme temperature and precipitation informs policy and decision makers about some of the most damaging aspects of anthropogenic global warming. In part 1 of this pair of papers comparing the early contributions to the phase 6 of the Coupled Model Intercomparison Project (CMIP6) to the previous phase (CMIP5), the performance of the two generations of climate models in simulating long period return values of daily precipitation and temperature were evaluated against gridded observations. The broad conclusion in that part of this study is that there is little difference between these two climate model databases in their ability to simulate this aspect of the present climate.

However, some of the models in the CMIP6 are characterized by very high climate sensitivity, the response of simulated temperature to increases in greenhouse gas (GHG) forcing (Zelinka et al., 2020). As a consequence, multi-model projections of future climate change at specified future times could be very different between CMIP5 and CMIP6. Since the 2016 Paris Agreement, much attention has been directed towards "target" stabilized global mean temperatures (UNEP, 2019). These global warming targets provide policy relevant information to the reduction and eventual elimination of greenhouse gas emissions. A recent special report of the Intergovernmental Panel on Climate Change focussed on the difference in impacts between a climate stabilized at 1.5C above preindustrial temperatures compared to a stable climate a half degree warmer (IPCC, 2018). For instance, increases in the severity and/or duration extreme heat events that lead to human mortality would be reduced under dramatic reductions in emissions (Lo et al., 2019) as would be the incidence of wildfires (Shiogama et al., 2020). However, even if the GHG emission reductions of the Paris Agreement's "National Determined Contributions" were achieved, global mean temperature would *very likely* exceed 1.5C and *likely* exceed 2.0C at 2 100 (DeAngelo et al., 2017). Also, as the NDC's are not zero emission targets, the climate would thereafter continue to warm if other actions to eliminate GHG emissions entirely are not put in place. Hence, it is appropriate to also examine the impacts of higher temperature targets as projected by climate models.

Projections of 20 year return values of daily extreme temperature and precipitation from the CMIP5 models for the 4 most commonly considered Representative Concentration Pathways (RCP) have been previously presented (Collins et al., 2013; Kharin et al., 2013) at mid (2046–2065) and end of (2081–2 100) the 21st century relative to a then recent reference period (1986–2005). In this study, we frame projections differently by considering the changes at specified global warming target temperatures of 1.5, 2, 3 and 4C above "preindustrial" levels. To be consistent with the forthcoming 6th IPCC Assessment Report, we define preindustrial as the 1851–1900 average as most of the observed global warming since the 18th century Industrial Revolution in Europe and elsewhere has occurred since 1900.

As different climate models exhibit a wide range of climate sensitivity (Vial et al., 2013), the point in time when global mean temperature change targets are reached varies considerably. High climate sensitivity models will reach specified targets earlier than low climate sensitivity models. Some low climate sensitivity models may not reach the higher targets at all prior to 2100, the common endpoint of the CMIP scenario experiments. Table 1 shows the dates when the targets are reached for the 24 CMIP6 models used in this study under three Shared Socioeconomic Pathways (SSP) scenarios, SSP245, SSP370 and SSP585.

E-mail address: mfwehner@lbl.gov.

https://doi.org/10.1016/j.wace.2020.100284
Received 28 December 2019; Received in revised form 19 June 2020; Accepted 8 September 2020
Available online 12 September 2020

Table 1
Year that CMIP6 models reach target warming levels by SSP scenario. "x" means that a particular scenario was not available. "-" means that the target warming level was not reached.

Model	1.5			2			3			4		
	ssp245	ssp370	ssp585	ssp245	ssp370	ssp585	ssp245	ssp370	ssp585	ssp245	ssp370	ssp585
ACCESS-CM2	2028	2027	2025	2040	2039	2038	2071	2062	2055	–	2082	2072
ACCESS-ESM1-5	2029	2033	2027	2045	2048	2039	–	2069	2060	–	–	2078
AWI-CM-1-1-MR[d]	2020	2022	x	2039	2037	x	–	2064	x	–	–	x
BCC-CSM2-MR	2035	2032	2030	2057	2046	2043	–	2074	2065	–	–	–
CESM2[a]	2026	2025	2024	2041	2041	2035	2081	2066	2053	–	2084	2069
CNRM-CM6-1	2030	2032	2028	2048	2045	2040	2084	2066	2058	–	2083	2072
CNRM-CM6-1-HR	x	x	2018	x	x	2029	x	x	2052	x	x	2066
CNRM-ESM2-1	2037	2036	2032	2055	2052	2045	2088	2072	2064	–	2089	2079
CanESM5	2013	2013	2012	2024	2023	2022	2049	2043	2040	2083	2059	2054
EC-Earth3	2022	2022	2024	2044	2038	2035	2085	2063	2057	–	2084	2073
EC-Earth3-Veg	2010	2011	2011	2033	2032	2027	2067	2057	2050	–	2076	2067
GFDL-CM4[d]	2031	x	2029	2049	x	2041	–	x	2059	–	x	2079
GFDL-ESM4	2046	2041	2039	2073	2057	2052	–	2083	2075	–	–	–
INM-CM4-8	2035	2035	2030	2063	2052	2046	–	2083	2069	–	–	–
INM-CM5-0	2037	2032	2030	2072	2050	2046	–	2084	2074	–	–	–
IPSL-CM6A-LR[b]	2018	2019	2018	2033	2034	2034	2065	2055	2050	–	2076	2066
MIROC6	2046	2043	2040	2073	2059	2053	–	–	2076	–	–	–
MPI-ESM1-2-HR	2037	2034	2033	2063	2050	2049	–	2081	2073	–	–	–
MPI-ESM1-2-LR	2036	2035	x	2057	2052	x	–	2078	x	–	–	x
MRI-ESM2-0[c]	2030	2031	2026	2049	2045	2038	–	2073	2064	–	–	2083
NESM3	x	x	2020	x	X	2033	x	x	2054	x	x	2072
NorESM2-LM	2055	2051	2042	2085	2069	2056	–	–	2077	–	–	–
NorESM2-MM	2045	2046	2039	2078	2062	2054	–	2090	2076	–	–	–
UKESM1-0-LL	2023	2022	2023	2034	2031	2031	2059	2050	2046	2090	2069	2060
CMIP6 average	**2031**	**2030**	**2027**	**2053**	**2046**	**2040**	**2072**	**2069**	**2061**	**2086**	**2077**	**2070**

[a]Rx1day only. [b]Rx1day, TNn, TNx only. [c]TNn, TNx only, [d]TNn, TNx, TXn, TXx only.

Table 2 show these dates for the 21 CMIP5 models used in this study under the RCP85 scenario (Hauser and Fischer, 2019). For this particular selection of models, the multi-model averaged dates at which the selected global warming targets are reached are roughly the same for both generations of models under the high emissions scenarios, RCP85 and SSP585 despite the wider range of climate sensitivities of the CMIP6 models. Extreme temperature and precipitation statistics are calculated for each model and scenario individually over a 20 year period extending from 10 years prior and 9 years after the years in these tables.

Table 2
Year that CMIP5 models reach target warming levels under the RCP8.5 scenario. "-" means that the target warming level was not reached.

	Warming level			
Model	1.5	2	3	4
ACCESS1-0	2027	2040	2060	2080
ACCESS1-3[b]	2030	2042	2061	2081
CCSM4	2014	2030	2057	2078
CESM1-BGC[c]	2017	2033	2059	2080
CMCC-CESM[d]	2037	2047	2067	2086
CMCC-CM	2029	2041	2061	2078
CMCC-CMS[e]	2029	2041	2061	2077
CNRM-CM5[b]	2030	2045	2067	2087
IPSL-CM5A-LR	2010	2026	2047	2065
IPSL-CM5A-MR	2015	2030	2050	2066
IPSL-CM5B-LR[b]	2022	2037	2061	2084
MIROC-ESM	2020	2030	2052	2069
MIROC-ESM-CHEM	2018	2030	2050	2067
MIROC5	2033	2048	2072	–
MPI-ESM-LR	2017	2037	2061	2081
MPI-ESM-MR[b]	2020	2039	2060	2082
MRI-CGCM3	2041	2052	2076	–
NorESM1-M	2032	2049	2073	–
bcc-csm1-1	2019	2036	2059	2083
bcc-csm1-1-m[d]	2010	2028	2059	2085
inmcm4	2044	2057	2083	–
cmip5 average	**2024**	**2038**	**2061**	**2078**

* [a]Rx1day only. [b]Rx1day, TNn, TNx only. [c]TNn, TNx only. [d]TXx, TXn only. [e]TNn, TNx, TXx, TXn only.

For the CMIP6 models, statistics are calculated first by scenario and subsequently averaged over relevant scenarios at the times in the tables to characterize the individual models at a specified global warming levels. Results are then presented separately for the CMIP5 and CMIP6 models as equally weighted multi-model averages for each global warming target.

The range of model climate sensitivities, reflected in the range of dates in Tables 1 and 2, introduces cross model uncertainty in projected climate statistics for a particular time and scenario simply due to the difference in simulated temperature changes. By considering fixed global temperature change targets, this source of uncertainty is transferred from the projected changes in the values of the actual metrics considered, say average annual precipitation maxima, to the uncertainty in the timing of the target. However, other important sources of uncertainty remain. Differences in the forced responses of the equator to pole temperature gradient and of the land/sea temperature differences lead to uncertainty in local mean temperature causing uncertainty in nearly any other aspect of local projections. Furthermore, the range of biases in models' mean climatologies as well as differences in process representation also lead to projection uncertainty in general, including that of extreme temperature and precipitation. Homogenization of the global mean temperature change then highlights these model differences. However, there is an important caveat to state when using output from transient climate model simulations as a proxy for stabilized warmer climate targets. The lag in ocean warming due to the long time scales of deep ocean mixing means that the land surface temperatures in a transient simulation at a specified global warming target would be warmer than in a stable simulation at that same global mean warming level. As this study considers changes in extreme temperatures and precipitation only over land from the non-stationary SSP and RCP scenarios, results would be slightly different if the models were integrated to a long stable climate. To the extent that temperature and precipitation extremes over land are influenced by local temperatures, these projected changes may be slightly larger than in such stabilized simulations (Mitchell et al., 2017; Wehner et al., 2018).

2. Data and methods

As in Part 1 of this pair of papers, we focus on selected indices from the Expert Team on Climate Change Detection Indices (ETCCDI) that are "block" maxima. "Hot days" are represented by *TXx*, the annual maximum of the daily maximum temperature. "Warm nights" are represented by *TNx*, the annual maximum of the daily minimum temperature. "Cool days" are represented by *TXn*, the annual minimum of the daily maximum temperature. "Cold nights" are represented by *TNn*, the annual minimum of the daily minimum temperature. "Wet days" are represented by *Rx1day*, the annual maxima of daily total precipitation. The indices are constructed from the daily maximum and minimum surface air temperatures and daily precipitation totals extracted from the CMIP5 and CMIP6 data archives. Values for the past are taken from the historical experiments and values for the future are taken from the CMIP5 RCP4.5, RCP6.0, RCP8.5 and the CMIP6 SSP245, SSP370 and SSP585 emission scenario experiments. Hence, projected changes in annual averages of 4 extreme temperature and 1 extreme precipitation variables and their long period (twenty year) return values are presented at four different warming levels.

Also as in Part 1, long period return values of daily temperatures and precipitation are estimated by fitting a non-stationary Generalized Extreme Value (GEV) distribution using $ln(CO_2)$ as a covariate representing anthropogenic climate change to long segments of the available model daily output (Coles, 2001). GEV distribution parameters are fitted using a Maximum Likelihood Estimates (MLE) procedure from the climextRemes software package (Paciorek et al., 2018), a python and R library built upon the extRemes library (Gilleland and Katz, 2016, 2011) and is available at https://cran.r-project.org/web/packages/climextRemes/index.html. The covariate appears linearly in the GEV location parameter as $\mu(t) = \mu_0 + \mu_1 ln(CO_2)$. Hence, there are four fitted parameters, the two components of the location parameter, μ_0, μ_1, the scale parameter σ and the shape parameter ξ. Twenty year return values defining the preindustrial reference are calculated by fitting the entire

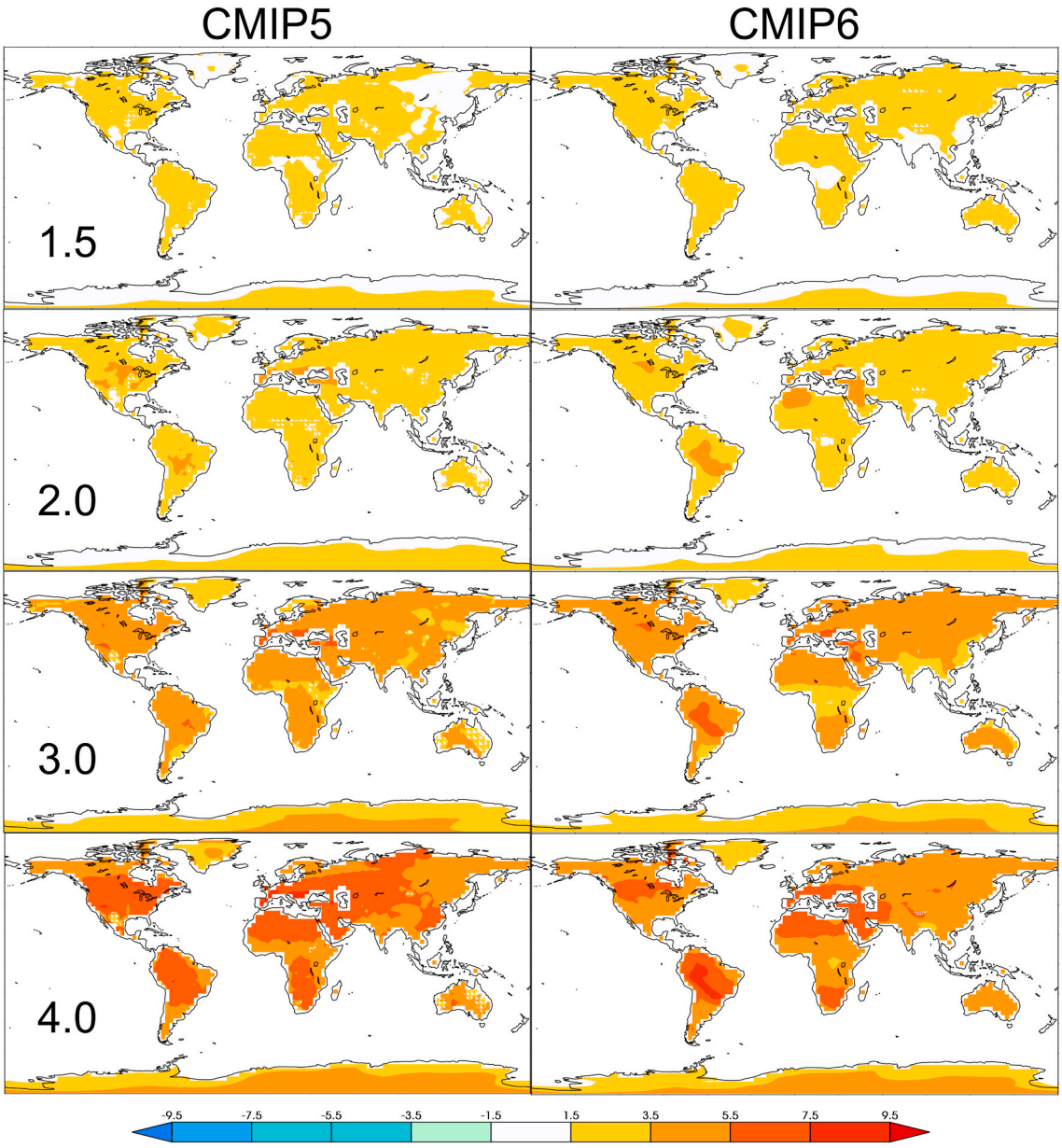

Fig. 1. Multimodel average projected changes in annual *TXx* (hot days) from available CMIP5 (left) and CMIP6 (right) at global warming levels of 1.5, 2, 3 and 4C above preindustrial (1850–1900) average values. Hatching indicates that the magnitudes of the multimodel projections are less than the cross-model standard deviation of the projections. Units: ^{o}C.

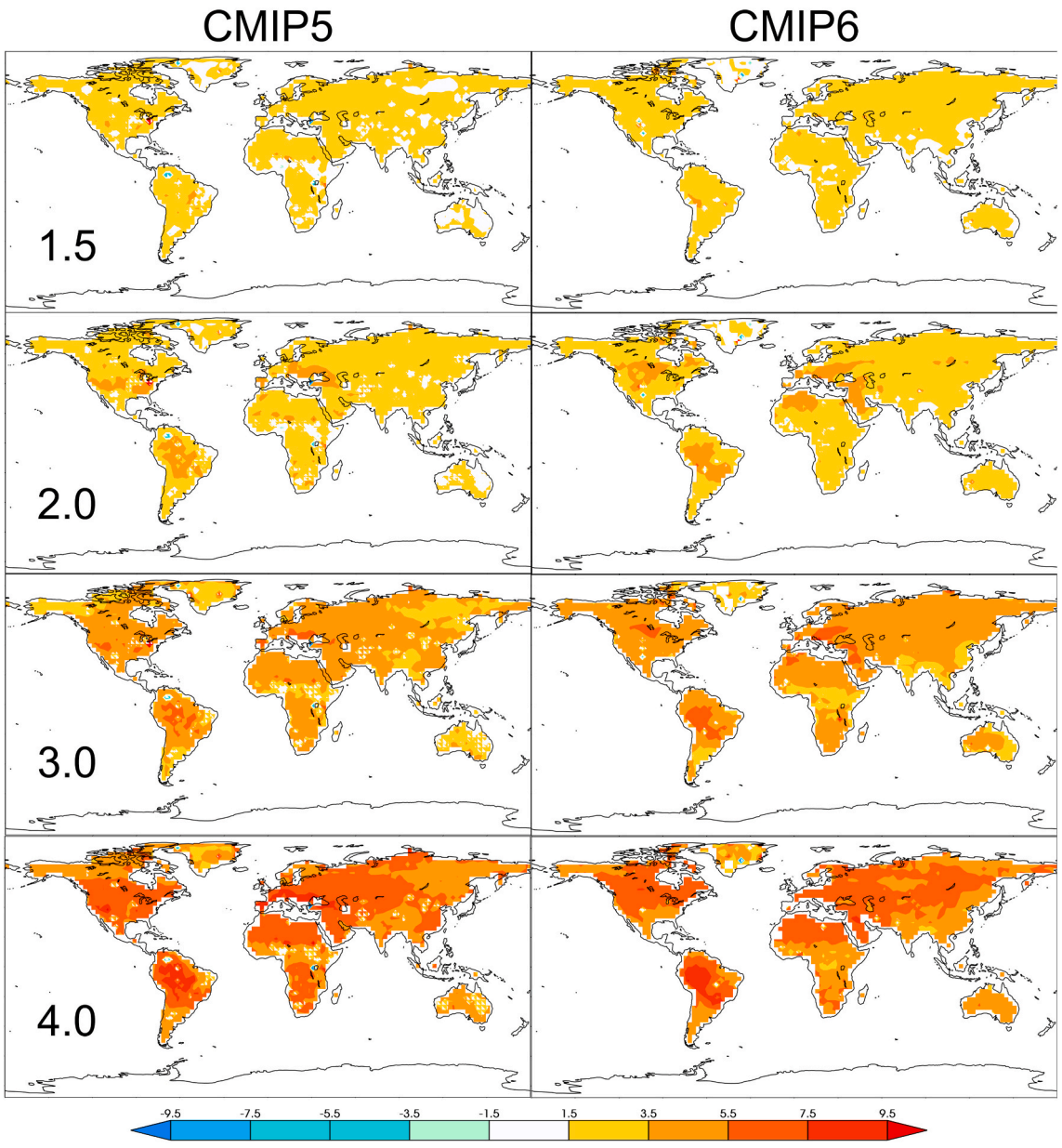

Fig. 2. Multimodel average projected changes in 20 year return values of *TXx* (very hot days) from available CMIP5 (left) and CMIP6 (right) at global warming levels of 1.5, 2, 3 and 4C above preindustrial (1850–1900) average values. Hatching indicates that the magnitudes of the multimodel projections are less than the cross-model standard deviation of the projections. Units: ^{o}C.

"historical" experiment (usually 1851–2013 for CMIP6 and 1851–2005 for CMIP5) using all ensemble members and averaging results over the 1851–1900 period. 20 year return values at the global warming targets are then estimated by fitting each SSP or RCP8.5 scenario experiment separately and in its entirety (usually 2016–2099 for CMIP6 and 2006–2099 for CMIP5) and using each available ensemble member as replicates. Note that μ_0, σ and ξ are the same for any year of a model's individual historical or scenario experiment but not required to be the same between experiments. Results at the global warming targets are then extracted from each scenario and combined as discussed above and the differences from the preindustrial reference calculated for each model. Alternatively, global mean temperature change since preindustrial could also be used as a covariate and changes in return values (but not the average of the extreme indices) extracted directly without calculating the timing of the global warming levels. Multi-model averages are performed as a final step by regridding to the coarsest available model (the 2.8^{o} CanESM5). As in part 1, projected changes in both the average annual indices (i.e. the 1 year return value) and their 20 year return values are presented to illustrate the effect of event rarity. Finally, in the maps of projected changes shown below, a simple hatching scheme, invoked where the magnitudes of the projections are less than the cross-model standard deviation of the projections, is used to illustrate a level of model agreement.

3. Temperature

3.1. Hot days

Fig. 1 shows projected multi-model changes in annual *TXx* (hot days) for available CMIP5 (left) and CMIP6 (right) models at global warming levels at 1.5, 2, 3 and 4C above average preindustrial (1850–1900) levels as defined by the 20 year intervals of Tables 1 and 2 This result plainly

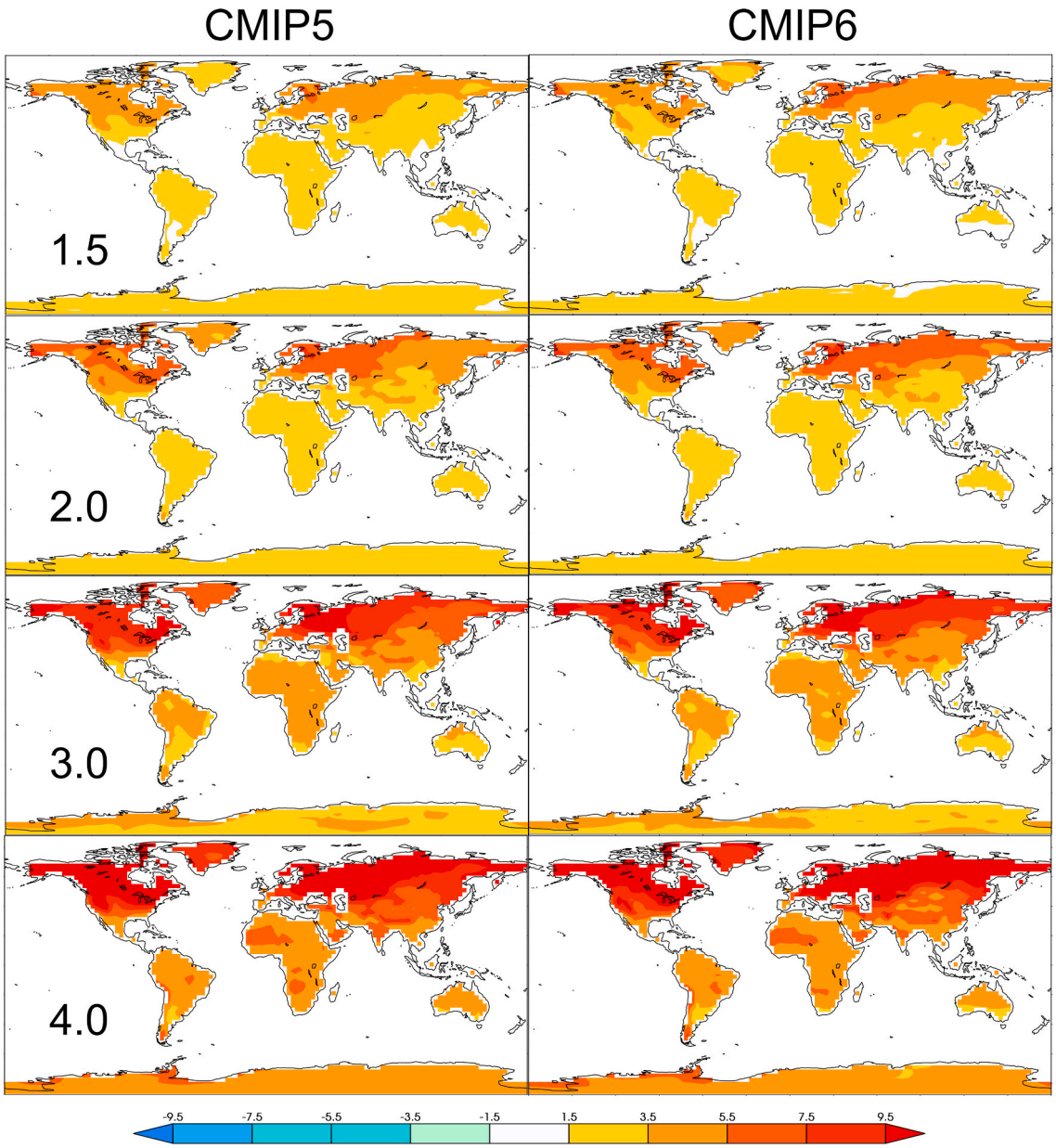

Fig. 3. Multimodel average projected changes in annual *TNn* (cold nights) from available CMIP5 (left) and CMIP6 (right) at global warming levels of 1.5, 2, 3 and 4C above preindustrial (1850–1900) average values. Hatching indicates that the magnitudes of the multimodel projections are less than the cross-model standard deviation of the projections. Units: ^{o}C.

illustrates that removing model differences in climate sensitivity by framing projections in terms of global warming levels as discussed in the previous section significantly reduces model differences in the magnitude of changes. The global land average change of annual *TXx* is slightly (10–20%) larger than each selected global warming level and reflects the difference in land and ocean warming that results by construction from transient rather than lengthy stabilized simulations. However, maximum warming amounts are about twice the selected global warming levels. No land regions exhibit cooling of annual *TXx* in either multimodel average. Also, few land regions are hatched indicating that the projected changes in annual *TXx* are quite large compared to cross model variability. As discussed below, the differences between the model generations at the 4C global warming level in average annual *TXx* changes is the largest of the eight temperature metrics discussed in this paper. However, the global average of this difference (~0.5C) is small compared to the global average change (~5C) and is much smaller at lower global warming levels.

Similarly, Fig. 2 shows projected multi-model changes in 20 year return values of annual *TXx* (very hot days) for the same set of available CMIP5 and CMIP6 models at the selected global warming levels. Despite the much larger magnitude of the 20 year return value of *TXx* than its annual average value, the projected future changes do not significantly differ between them. Like the annual *TXx* changes, the global land average changes in its 20 year return value are about the same magnitude in each model generation and slightly larger than the selected global warming levels. Maximum return value warmings are larger than the maximum annual warmings but tend to be small isolated regions reflecting statistical fit uncertainties or internal variability rather than anything physically meaningful. Stability of changes in extreme hot temperatures across rarities ranging from 20 to 100 year return values had been noted previously in comparing results from stationary climate model simulations (Wehner et al., 2018) and attributed to the shape of the bounded GEV distributions (Coles, 2001). This stability in hot day temperature changes extends to 1 year return values and non-stationary

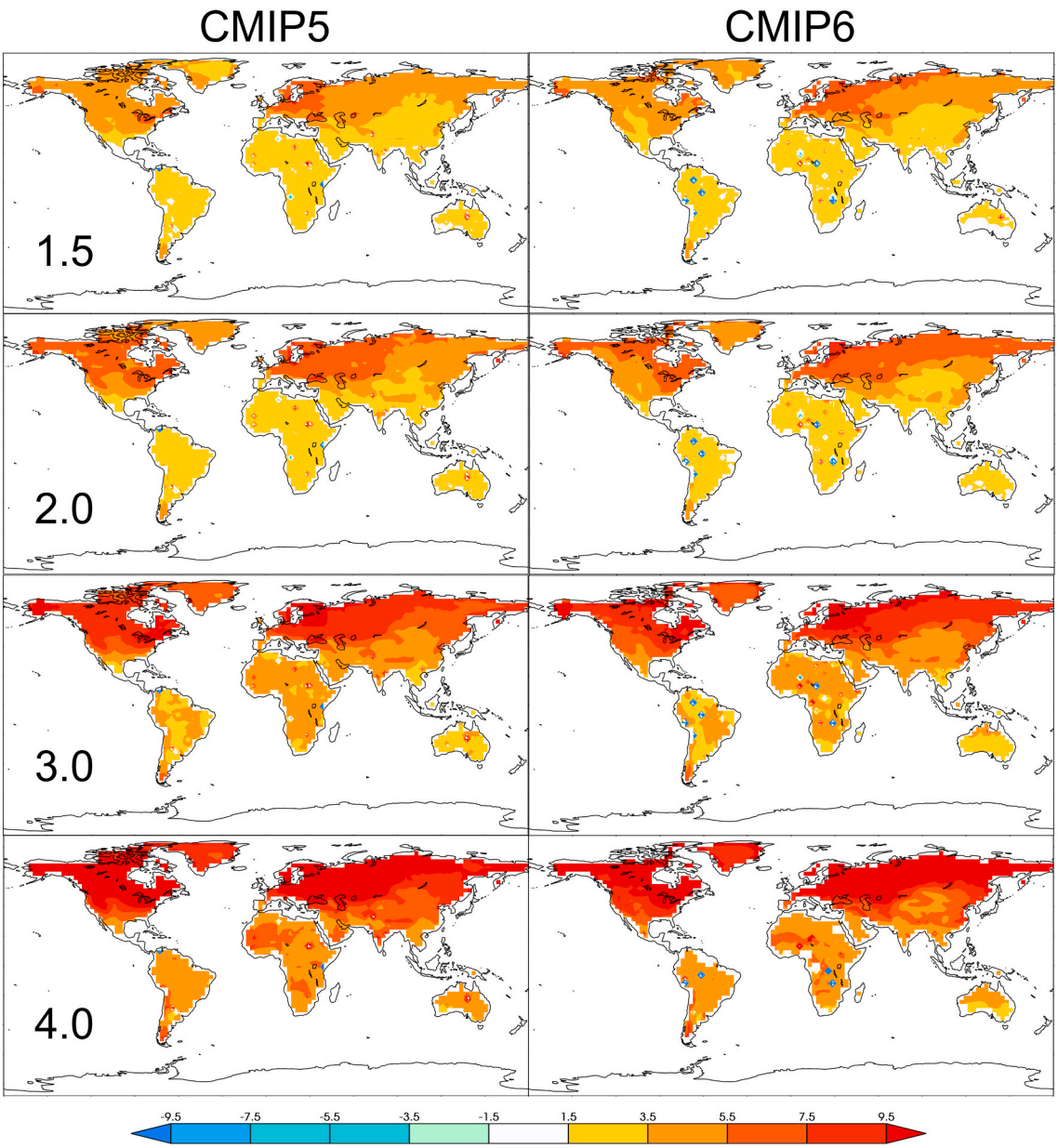

Fig. 4. Multimodel average projected changes in 20 year return values of *TNn* (very cold nights) from available CMIP5 (left) and CMIP6 (right) at global warming levels of 1.5, 2, 3 and 4C above preindustrial (1850–1900) average values. Hatching indicates that the magnitudes of the multimodel projections are less than the cross-model standard deviation of the projections. Units: °C.

simulations. While this stability would be expected in the asymptotic limit of large return values from two bounded GEV distributions, the fact that it happens at such low levels of rarity means that the shape and scale parameters from the historical and future simulations are very similar. Here, this is not guaranteed as the historical and each future scenario are fit to the GEV parameters independently.

As for projected changes in annual *TXx*, differences between CMIP5 and CMIP6 projected changes in 20 year return values of *TXx* are minor and not systematic with large scale differences only being apparent on this color scale at the 4C global warming level. In this case, the global average of this difference is very smaller (~0.03C) compared to the global average change (~5C).

3.2. Cold nights

Fig. 3 shows projected multi-model changes in annual *TNn* (cold nights) for available CMIP5 (left) and CMIP6 (right) models at the specified global warming levels. As in previous studies framing projected changes at specified times and emissions scenarios (Collins et al., 2013; Kharin et al., 2013; Sillmann et al., 2013), projected changes in cold nights are larger than changes in hot days. Global land average changes in annual *TNn* range from 90% (1.5C target) to 70% (4C target) larger than the specified global warming levels. High latitudes warm more than low latitudes suggestive of surface albedo feedbacks associated with melting of snow cover as average temperatures rise (Fischer et al., 2011). As with hot days, there are no meaningful differences between the CMIP5 and CMIP6 ensembles and all projected changes are larger than the cross model standard deviations and no cells are hatched.

Fig. 4 shows projected multi-model changes in 20 year return values of annual *TNn* (very cold nights) for the same set of available CMIP5 and CMIP6 models at the selected global warming levels. A few models exhibited pointwise fitting failures that propagate into the multi-model average changes, mostly in Africa and South America. In the well characterized cells, changes in the 20 year return value of *TNn* and in its

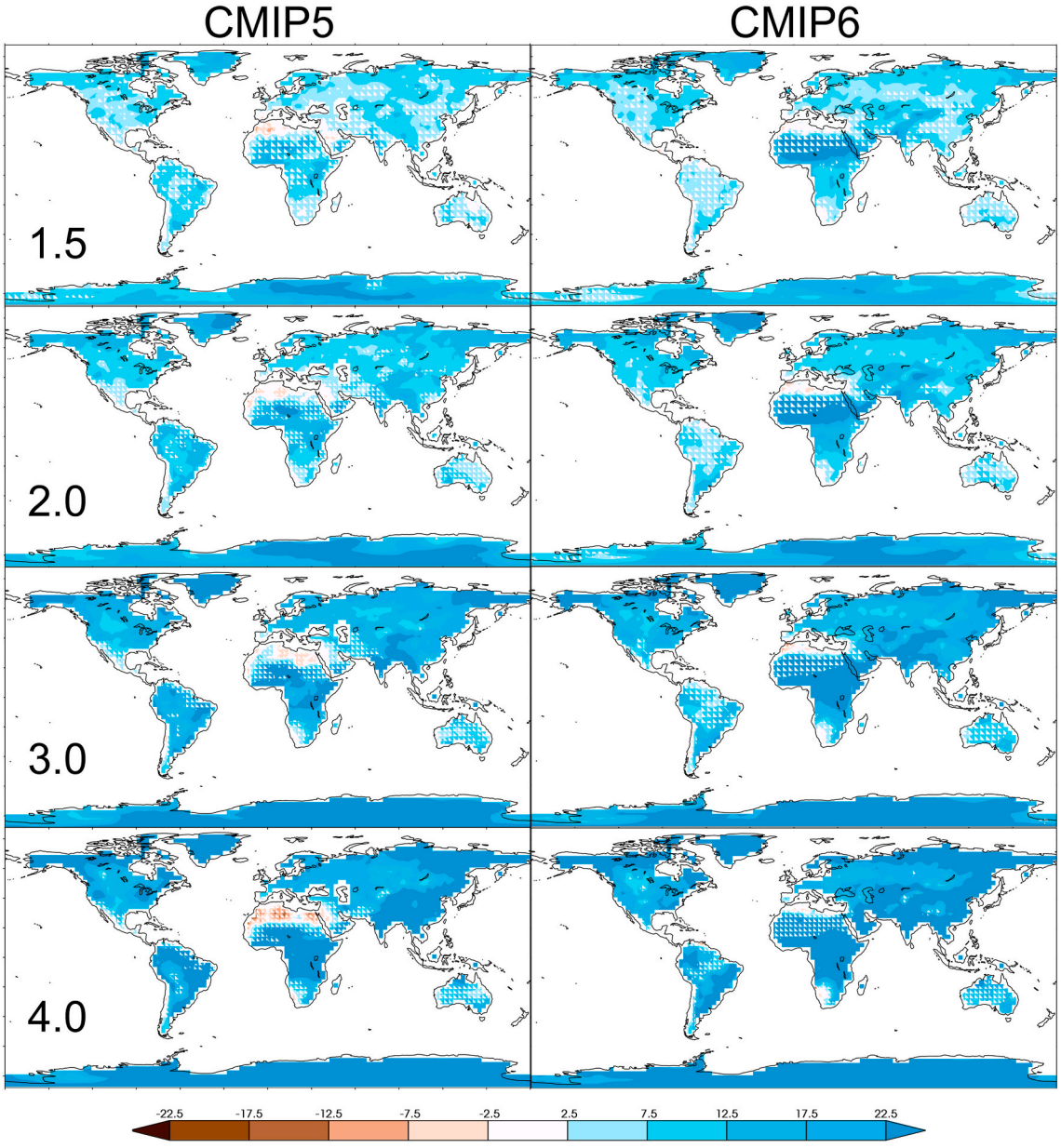

Fig. 5. Multimodel average projected percent changes in annual *Rx1day* (wet days) from available CMIP5 (left) and CMIP6 (right) at global warming levels of 1.5, 2, 3 and 4C above preindustrial (1850–1900) average values. Hatching indicates that the magnitudes of the multimodel projections are less than the cross-model standard deviation of the projections. Units: percent.

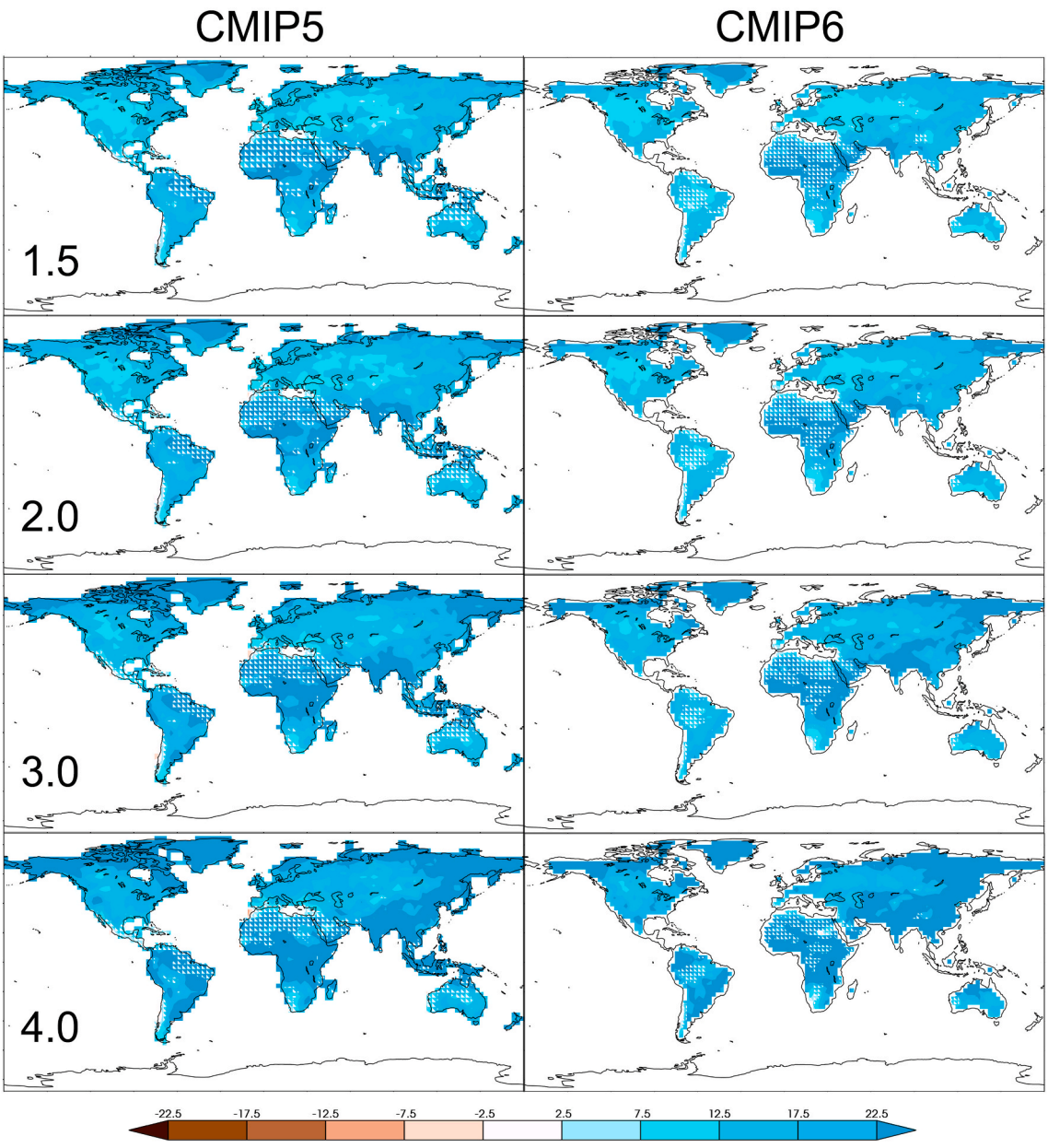

Fig. 6. Multimodel average projected percent changes in 20 year return values of *Rx1day* (very wet days) from available CMIP5 (left) and CMIP6 (right) at global warming levels of 1.5, 2, 3 and 4C above preindustrial (1850–1900) average values. Hatching indicates that the magnitudes of the multimodel projections are less than the cross-model standard deviation of the projections. Units: percent.

Table 3
Comparison of CMIP5 and CMIP6 multi-model average extreme temperature and precipitation changes over land at the 4C above pre-industrial warming level. Middle column: Centered pattern correlation between CMIP5 and CMIP6. Right column: Difference in global mean between CMIP5 and CMIP6.

	correlation	CMIP5-CMIP6
Rx1day	0.51	−5.16%
Rx1day RV	0.44	−3.59%
TNx	0.92	−0.11C
TNx RV	0.32	0.00C
TNn	0.96	−0.01C
TNn RV	0.85	0.10C
TXn	0.98	−0.15C
TXn RV	0.86	0.14C
TXx	0.80	0.45C
TXx RV	0.24	0.03C

Table 4
Relationships between changes at the 4C above pre-industrial warming level in the average value of the extreme indices and their twenty year return values for the CMIP5 and CMIP6 models over land. Columns labelled "correlation" show the centered pattern correlation between the average change and the return value change. Columns labelled "RV-index" show the difference between the twenty year return value changes and the changes in the average value of the indices.

	CMIP6		CMIP5	
	correlation	RV-index	correlation	RV-index
TNx	0.57	0.11C	0.61	0.22C
TNn	0.93	0.35C	0.95	0.47C
TXx	0.70	0.55C	0.45	0.13C
TXn	0.93	0.13C	0.94	0.43C
Rx1day	0.82	−1.23%	0.63	0.34%

annual average value are again very close in magnitude illustrating stability of changes across rarity of cold day frequency due the bounded nature of the GEV distribution. Again, meaningful differences between CMIP5 and CMIP6 are difficult to identify with most large scale differences again being apparent on this color scale only at the 4C global warming level. In this case, the global average of this difference is yet smaller (~0.1C) compared to the global average change (~7C).

Projection maps of changes in warm nights and cool days are presented in the appendix but discussed with the other extreme temperature projections in section 5.

4. Precipitation: wet days

Fig. 5 shows projected multi-model percent changes in annual *Rx1day* (wet days) for available CMIP5 (left) and CMIP6 (right) models at the specified global warming levels. Hatching indicates that at the lower global warming targets, projected changes in extreme precipitation are not as robustly larger than cross model variations than at the higher targets. There is little evidence in Fig. 5 to suggest that CMIP5 and CMIP6 projected changes in annual *Rx1day* are meaningfully different.

Fig. 6 shows projected multi-model percent changes in 20 year return values of annual *Rx1day* (very wet days) for the CMIP5 and CMIP6 models at the selected global warming levels. The projected increases in annual *Rx1day* return values are remarkably similar to annual *Rx1day* itself. Again, the hatched areas where projected percent changes are less than cross model standard deviation are small for both model ensembles and all warming levels. Projected return values changes are positive everywhere with increases for both ensembles as global warming targets increase. This even includes the CMIP6 projections at 1.5 and 2C targets.. The hatched areas of less robust projected changes are confined to the dry regions of the land mass (the Sahara, northeastern Brazil and part of Australia).

5. Discussion

Confidence in projected changes in extreme temperature and precipitation in a future warmer climate is limited both by confidence in the quality of simulations of the contemporary climate as well as in model representation of the known physical mechanisms affected by climate change. For a given change in greenhouse gas concentration, the leading source of uncertainty in most, if not all, climate change projections is "climate sensitivity", the temperature response of the climate system to a change in atmospheric composition (Hawkins and Sutton, 2009). In this paper, to inform a decision about the presentation of future changes in extreme temperature and precipitation by the lead authors of the forthcoming 6th Assessment Report of Working Group One of the Intergovernmental Panel on Climate Change (IPCC WG1 AR6), projections of extreme daily temperature and precipitation changes are framed in terms of four specified global warming targets rather than by individual emissions scenarios over specified time intervals. The area hatched as uncertain in maps of projections made at global warming target levels is reduced compared to projections maps made at equivalent specified times and emission scenarios regardless of the scheme to measure multi-model uncertainty. However, this reframing does not eliminate the large uncertainty from differences in model climate sensitivity. Rather it simply shifts this model structural uncertainty to the timing of when a target is reached.

This reframing reveals that there are no meaningful differences in future multi-model projections of changes in extreme temperature and precipitation between the mature CMIP5 and the as yet still underway CMIP6 ensembles other than that arising from differences in the range of climate sensitivities. Furthermore, as shown in the first of these two companion papers, there is no meaningful difference in the quality of simulated extreme temperature and precipitation when formally evaluated against available observations. Table 3 presents a summary of the relationships between CMIP5 and CMIP6 multi-model average projected changes at the 4C above preindustrial global warming level. Differences between the two generations of models are larger at this warming level than at the lower levels considered here. Differences in the magnitude of changes are small for all the temperature indices and their return values except hot days (*TXx*) where the CMIP5 multimodel average is about a 0.5C warmer than CMIP6 (out of a ~5° warming). Centered pattern correlations of the changes are high for all of the average extreme temperature indices and also for the return value changes of the cold temperature extremes. Pattern correlations of the return value changes of the warm extremes are low, but the global mean magnitudes are nearly the same. The two generations of models differ more in the extreme precipitation metrics with wetter changes in the CMIP6 multimodel average. Centered pattern correlations of extreme precipitation changes are moderate between CMIP5 and CMIP6. Despite the differences noted here, even the largest are less than the model uncertainty criterion used in the figures and would be hatched if similarly plotted.

This lack of meaningful differences between the two generations of climate models in their simulation quality and target projections permits them to be combined. It is then recommended to the lead authors of IPCC WG1 AR6 that projections of extreme temperature and precipitation changes be calculated in this way combining RCP4.5, RCP6.0 and RCP8.5 of CMIP5 with SSP245, SSP370 and SSP585 of CMIP6 to most fully utilize publicly available climate model output. In this way, projection uncertainty in this targeted framing will most fully sample the range of future changes.

This study also reveals that projected changes in long period return values of the four block maxima ETCCDI temperature indices, *TXx*, *TXn*, *TNn*, and *TNx* are insensitive to rarity as twenty year return value changes are not very different from the one year return value (i.e. the average of the indices) changes. As might be expected, multi-model changes in extreme temperatures from the coarse CMIP5/6 models are increases everywhere over land and increase as global average temperature increases. In fact, changes in the multi-model average of these indices, or the one year return value, may adequately inform the multimodel average of longer period return values, of any fixed rarity. Table 4 presents a summary of the relationship between twenty year return value changes and average changes over land in the for extreme temperature indices separately for the CMIP5 and CMIP6 multi-model averages at the 4C above preindustrial global warming level. All return value changes are warmer than the corresponding average extreme temperature changes, but as increases over land range from about 5 to 7C, these differences are small and well within cross model uncertainties. Centered pattern correlation between return value and average extreme changes are high for the cold temperature extremes and moderate for the warm temperature extremes for both generations of models. This insensitivity of temperature extreme changes are a property of the shape of bounded GEV cumulative distribution functions and little difference between past and future scale and shape parameters (Wehner et al., 2018). In this study, only the location parameters vary with time in the non-stationary GEV statistical formalism. However, separate GEV fits were made to the past and future segments of the model simulations for convenience as there are different numbers of realizations available for each CMIP subproject. Hence, the fitted scale and shape parameters are not prescribed to be the same for the past and future return value estimates although they are not particularly different. Nonetheless, there are reasons to consider that in some regions they should be non-stationary and functions of local mean temperature due to land surface feedbacks. As mean temperature increase, soils experience increased evapotranspiration and can become drier. The

resultant reduction in evaporative cooling is a potential mechanism for further increases in extreme temperatures. Due to the substantial differences in land component submodels in the CMIP models, there could also be substantial differences in their nonstationary properties of simulated extreme temperatures. Although out of scope for this study, further analysis could be revealing.

Projected percent changes in the extreme precipitation block maxima are also expected to depend on rarity. The saturated atmospheric conditions leading to extreme precipitation are controlled by the Clausius-Clapeyron (C–C) relationship of about 7% per degree (C) of local warming (Allen and Ingram, 2002). However, high resolution simulations and event attribution studies (Pall et al., 2017; Risser and Wehner, 2017; Scoccimarro et al., 2014; Van Oldenborgh et al., 2017; Wang et al., 2018) have indicated that very extreme precipitation can increase at super C–C rates, a result supported by observations (Lenderink et al., 2017) and theoretical understanding of how local and non-local changes in atmospheric dynamics can affect moisture convergence (O'Gorman and Schneider, 2009; Schneider et al., 2010). On the other hand, CMIP3 and CMIP5 models do not exhibit such super C–C scaling in extreme precipitation (Kharin et al., 2013, 2007). Table 3 and Figs. 5 and 6 show that the CMIP5 and CMIP6 global land average changes in *Rx1day* and its 20 year return value are very similar in pattern and magnitude unlike what would be expected under significant super C–C scaling. One reason for this is that the standard horizontal resolutions of the CMIP5 and CMIP6 models do not permit the strong temperature and moisture gradients characteristic of the severe storms such as tropical cyclones or mesoscale convective systems that produce extreme precipitation (Walsh et al., 2015; Wehner et al., 2015, 2014). Convective parameterization schemes may also constrain extreme precipitation (Li et al., 2011) as they are not generally tuned to replicate the tail of the distribution even at high resolutions (Yang et al., 2012). In principle, permitting the scale parameter to be non-stationary via a dependence on $ln(CO_2)$ or temperature might both improve the quality of fit and accentuate the differences in the changes in extreme precipitation of different rarities. This would provide another important performance metric to validate climate models with but is a task for future work.

This paper and its companion paper question the added benefit of the CMIP6 to enhancing confidence in projected changes to extreme temperature and precipitation. The model errors in simulated available global observations remain substantial and users of CMIP5/6 are left to question whether this model output is fit for their purposes. Sources of model errors relevant to simulated extreme weather are many at this coarse horizontal resolution and range from large scale processes such as atmospheric blocking (Schiemann et al., 2017) and land processes (Mueller and Seneviratne, 2014) to smaller scale unresolved convection processes (Cole et al., 2005). Some classes of storms leading to extreme precipitation such as tropical cyclones are non-existent or at best unrealistic at the typical CMIP5/6 resolution of 100 km (Wehner et al., 2015). Further increases in our confidence in projected changes in extreme temperature and precipitation therefore will require a mix of higher resolution models and improvement in relevant parameterizations.

CRediT authorship contribution statement

Michael F. Wehner: Conceptualization, Methodology, Visualization.

Declaration of competing interest

The authors declare that they have no known competing financial interests or personal relationships that could have appeared to influence the work reported in this paper.

Acknowledgement

The research performed at Lawrence Berkeley National Laboratory was supported by the Director, Office of Science, Office of Biological and Environmental Research of the U.S. Department of Energy under Contract No. DE340AC02-05CH11231.. Support from the Regional and Global Climate Modeling program is gratefully acknowledged. This document was prepared as an account of work sponsored by the United States Government. While this document is believed to contain correct information, neither the United States Government nor any agency thereof, nor the Regents of the University of California, nor any of their employees, makes any warranty, express or implied, or assumes any legal responsibility for the accuracy, completeness, or usefulness of any information, apparatus, product, or process disclosed, or represents that its use would not infringe privately owned rights. Reference herein to any specific commercial product, process, or service by its trade name, trademark, manufacturer, or otherwise, does not necessarily constitute or imply its endorsement, recommendation, or favoring by the United States Government or any agency thereof, or the Regents of the University of California. The views and opinions of authors expressed herein do not necessarily state or reflect those of the United States Government or any agency thereof or the Regents of the University of California.

This work used resources at the National Energy Research Supercomputer Center (NERSC) at the Lawrence Berkeley National Laboratory. I acknowledge the World Climate Research Programme, which, through its Working Group on Coupled Modelling, coordinated and promoted CMIP5 and CMIP6. I thank the climate modeling groups for producing and making available their model output, the Earth System Grid Federation (ESGF) for archiving the data and providing access, and the multiple funding agencies who support CMIP6 and ESGF. I would also like to than Mathias Hauser (ETH Zurich) for his timely calculation of global warming level timings.

Appendix A. Supplementary data

Supplementary data to this article can be found online at https://doi.org/10.1016/j.wace.2020.100284.

Appendix

Fig. A1shows projected multi-model changes in annual *TNx* (warm nights) for available CMIP5 (left) and CMIP6 (right) models at the specified global warming levels. Changes in warm nights are very similar to changes in hot days. Similar to Fig. 1, changes in annual *TNx* are remarkably uniform, with continental interiors warming only slightly more than coastal regions for models at the coarse resolution of the standard CMIP5 and CMIP6 models. Also, as with the changes in very hot days, changes in the 20 year return value of annual *TNx* are very similar to changes in its annual value.

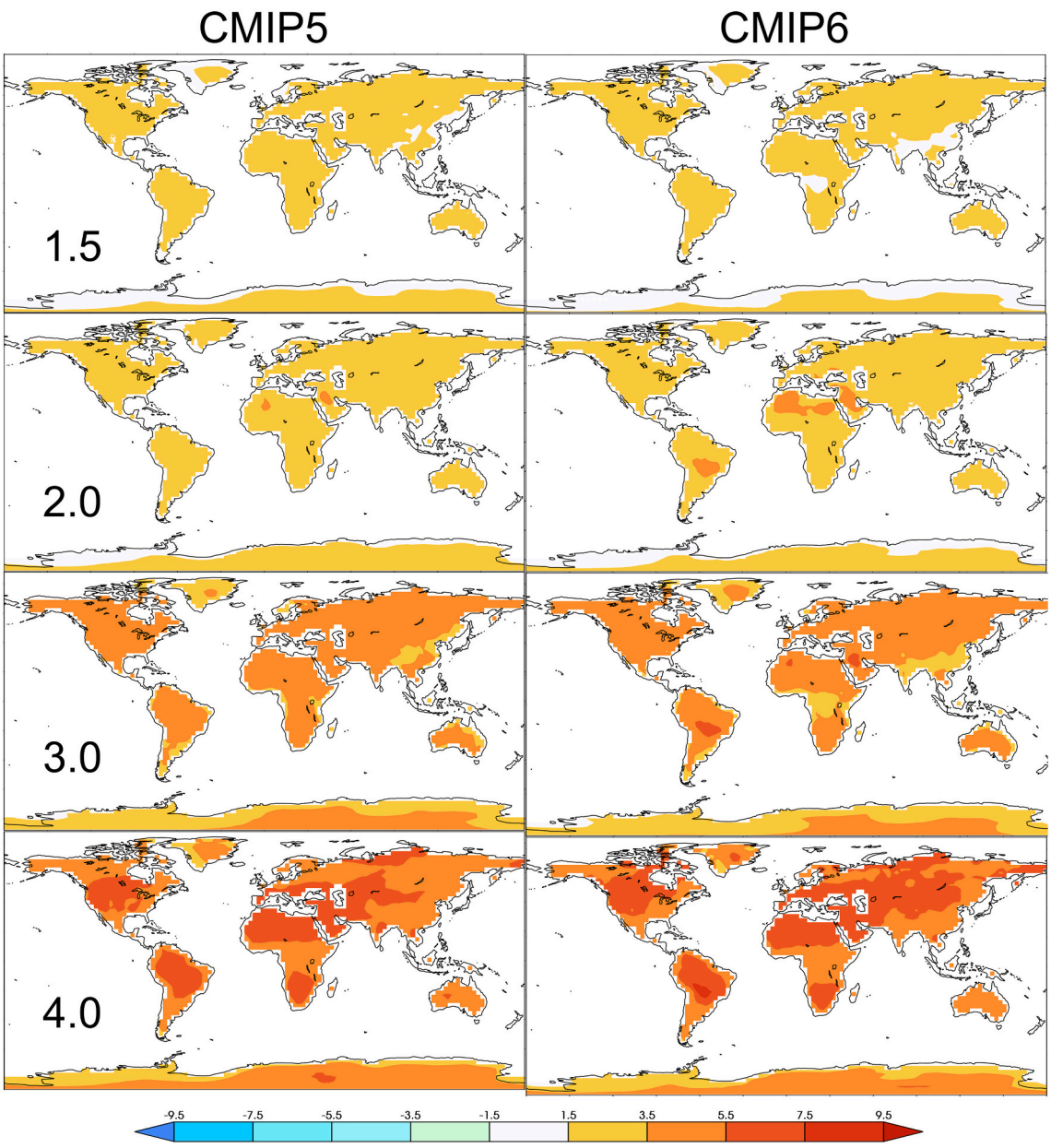

Fig. A1. Multimodel average projected changes in annual *TNx* (warm nights) from available CMIP5 (left) and CMIP6 (right) at global warming levels of 1.5, 2, 3 and 4C above preindustrial (1850–1900) average values. Units: °C.

Fig. A2 shows projected multi-model changes in annual *TXn* (cool days) for available CMIP5 (left) and CMIP6 (right) models at the specified global warming levels. Changes in cool days are very similar to changes in cold nights. Similar to Fig. 2, increases in annual *TXn* are largest at higher latitudes. Also, as with the changes in very cold nights, changes in the 20 year return value of annual *TXn* are very similar to changes in its annual value.

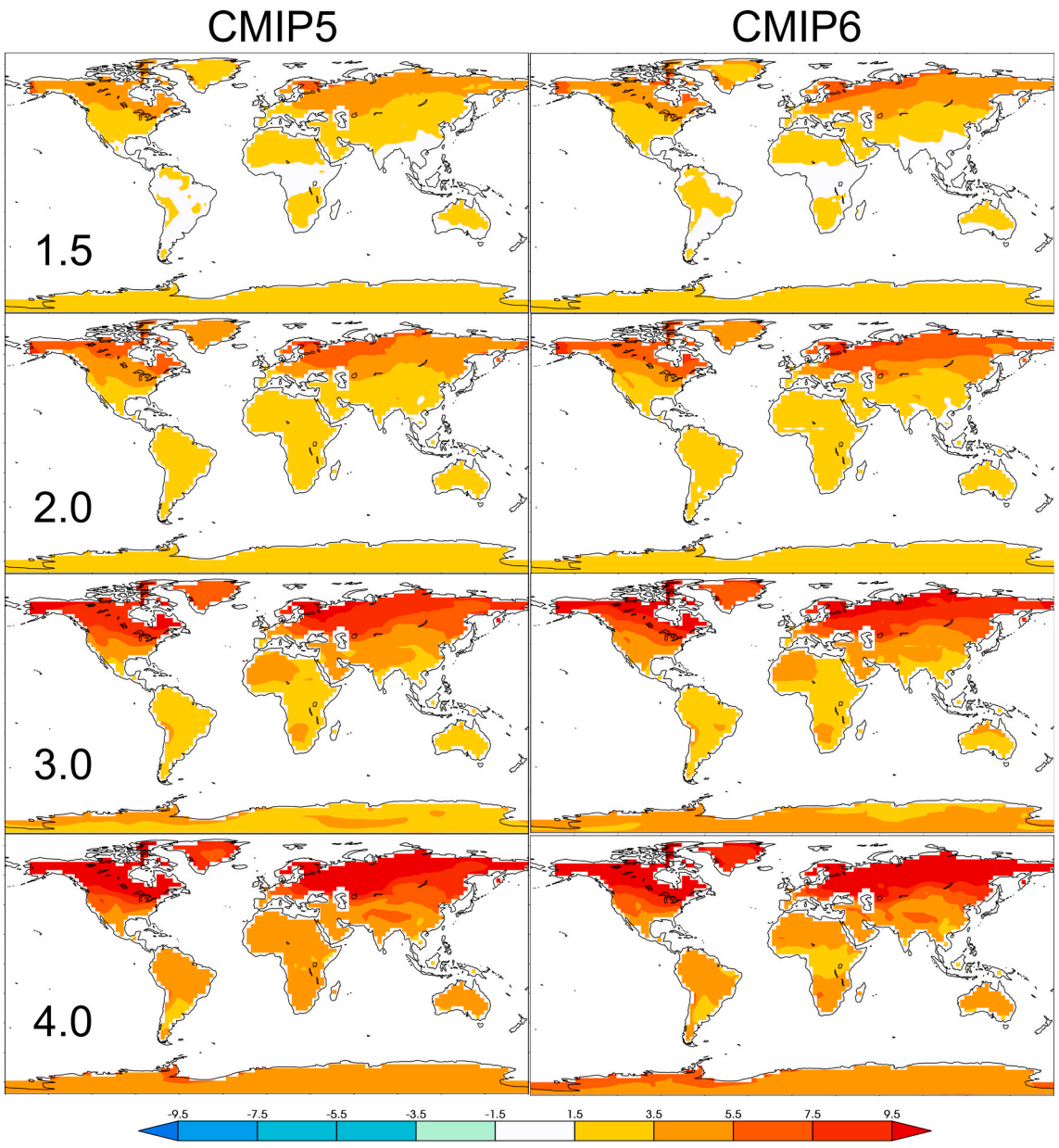

Fig. A2. Multimodel average projected changes in annual *TXn* (cool days) from available CMIP5 (left) and CMIP6 (right) at global warming levels of 1.5, 2, 3 and 4C above preindustrial (1850–1900) average values. Units: ^{o}C.

References

Allen, M.R., Ingram, W.J., 2002. Constraints on future changes in climate and the hydrologic cycle. Nature 419, 224–232. https://doi.org/10.1038/nature01092.

Cole, J.N.S., Barker, H.W., Randall, D.A., Khairoutdinov, M.F., Clothiaux, E.E., 2005. Global consequences of interactions between clouds and radiation at scales unresolved by global climate models. Geophys. Res. Lett. 32 https://doi.org/10.1029/2004GL020945.

Coles, S., 2001. An Introduction to Statistical Modeling of Extreme Values. In: Springer Series in Statistics. Springer.

Collins, M., Knutti, R., Arblaster, J., Dufresne, J.-L., Fichefet, T., Friedlingstein, P., Gao, X., Gutowski, W.J., Johns, T., Krinner, G., Shongwe, M., Tebaldi, C., Weaver, A. J., Wehner, M., 2013. Long-term climate change: projections, commitments and irreversibility. In: Stocker, T.F., Qin, D., Plattner, G.-K., Tignor, M., Allen, S.K., Boschung, J., Nauels, A., Xia, Y., Bex, V., Midgley, P.M. (Eds.), Climate Change 2013: the Physical Science Basis. Contribution of Working Group I to the Fifth Assessment Report of the Intergovernmental Panel on Climate Change. Cambridge University Press, Cambridge,, pp. 1029–1136. https://doi.org/10.1017/CBO9781107415324.024. United Kingdom and New York, NY, USA.

DeAngelo, B., Edmonds, J., Fahey, D.W., Sanderson, B.M., 2017. Perspectives on climate change mitigation. In: Wuebbles, D.J., Fahey, D.W., Hibbard, K.A., Dokken, D.J., Stewart, B.C., Maycock, T.K. (Eds.), Climate Science Special Report: Fourth National Climate Assessment, Volume I. U.S. Global Change Research Program, Washington,, pp. 393–410. https://doi.org/10.7930/J0M32SZG. DC, USA.

Fischer, E.M., Lawrence, D.M., Sanderson, B.M., 2011. Quantifying uncertainties in projections of extremes—a perturbed land surface parameter experiment. Clim. Dynam. 37, 1381–1398. https://doi.org/10.1007/s00382-010-0915-y.

Gilleland, E., Katz, R.W., 2011. New software to analyze how extremes change over time. Eos, Trans. Am. Geophys. Union 92, 13–14. https://doi.org/10.1029/2011EO020001.

Gilleland, E., Katz, R.W., 2016. extRemes 2.0: an extreme value analysis package in R. J. Stat. Software 1. https://doi.org/10.18637/jss.v072.i08. Issue 8.

Hauser, M., Fischer, E.M., 2019. Transient warming levels for CMIP5 and CMIP6. https://doi.org/10.5281/ZENODO.3591807.

Hawkins, E., Sutton, R., 2009. The potential to narrow uncertainty in regional climate predictions. Bull. Am. Meteorol. Soc. 90, 1095–1108. https://doi.org/10.1175/2009BAMS2607.1.

IPCC, 2018. Global warming of 1.5°C. An IPCC Special Report on the impacts of global warming of 1.5°C above pre-industrial levels and related global greenhouse gas emission pathways, in the context of strengthening the global response to the threat of climate change. The Intergovernmental Panel on Climate Change.

Kharin, V.V., Zwiers, F.W., Zhang, X., Hegerl, G.C., 2007. Changes in temperature and precipitation extremes in the IPCC ensemble of global coupled model simulations. J. Clim. 20, 1419–1444. https://doi.org/10.1175/JCLI4066.1.

Kharin, V.V., Zwiers, F.W., Zhang, X., Wehner, M., 2013. Changes in temperature and precipitation extremes in the CMIP5 ensemble. Climatic Change 119. https://doi.org/10.1007/s10584-013-0705-8.

Lenderink, G., Barbero, R., Loriaux, J.M., Fowler, H.J., 2017. Super-clausius–clapeyron scaling of extreme hourly convective precipitation and its relation to large-scale Atmospheric conditions. J. Clim. 30, 6037–6052. https://doi.org/10.1175/JCLI-D-16-0808.1.

Li, F., Collins, W.D., Wehner, M.F., Williamson, D.L., Olson, J.G., Algieri, C., 2011. Impact of horizontal resolution on simulation of precipitation extremes in an aqua-planet version of Community Atmospheric Model (CAM3). Tellus Ser. A Dyn. Meteorol. Oceanogr. 63 https://doi.org/10.1111/j.1600-0870.2011.00544.x.

Lo, Y.T.E., Mitchell, D.M., Gasparrini, A., Vicedo-Cabrera, A.M., Ebi, K.L., Frumhoff, P.C., Millar, R.J., Roberts, W., Sera, F., Sparrow, S., Uhe, P., Williams, G., 2019. Increasing mitigation ambition to meet the Paris Agreement's temperature goal avoids substantial heat-related mortality in U.S. cities. Sci. Adv. 5, eaau4373. https://doi.org/10.1126/sciadv.aau4373.

Mitchell, D., AchutaRao, K., Allen, M., Bethke, I., Beyerle, U., Ciavarella, A., Forster, P. M., Fuglestvedt, J., Gillett, N., Haustein, K., Ingram, W., Iversen, T., Kharin, V., Klingaman, N., Massey, N., Fischer, E., Schleussner, C.-F., Scinocca, J., Seland, Ø., Shiogama, H., Shuckburgh, E., Sparrow, S., Stone, D., Uhe, P., Wallom, D., Wehner, M., Zaaboul, R., 2017. Half a degree additional warming, prognosis and projected impacts (HAPPI): background and experimental design. Geosci. Model Dev. (GMD) 10. https://doi.org/10.5194/gmd-10-571-2017.

Mueller, B., Seneviratne, S.I., 2014. Systematic land climate and evapotranspiration biases in CMIP5 simulations. Geophys. Res. Lett. 41, 128–134. https://doi.org/10.1002/2013GL058055.

O'Gorman, P.A., Schneider, T., 2009. Scaling of precipitation extremes over a wide range of climates simulated with an idealized GCM. J. Clim. 22, 5676–5685. https://doi.org/10.1175/2009JCLI2701.1.

Paciorek, C.J., Stone, D.A., Wehner, M.F., 2018. Quantifying statistical uncertainty in the attribution of human influence on severe weather. Weather Clim. Extrem. 20, 69–80. https://doi.org/10.1016/j.wace.2018.01.002.

Pall, P., Patricola, C.M., Wehner, M.F., Stone, D.A., Paciorek, C.J., Collins, W.D., 2017. Diagnosing conditional anthropogenic contributions to heavy Colorado rainfall in September 2013. Weather Clim. Extrem. https://doi.org/10.1016/j.wace.2017.03.004.

Risser, M.D., Wehner, M.F., 2017. Attributable human-induced changes in the likelihood and magnitude of the observed extreme precipitation during hurricane harvey. Geophys. Res. Lett. https://doi.org/10.1002/2017GL075888.

Schiemann, R., Demory, M.-E., Shaffrey, L.C., Strachana, J., Vidale, P.L., Mizielinski, M. S., Roberts, M.J., Wehner, M.F., Jung, T., 2017. The resolution sensitivity of Northern Hemisphere blocking in four 25-km atmospheric global circulation models. J. Clim. 30 https://doi.org/10.1175/JCLI-D-16-0100.1.

Schneider, T., O'Gorman, P.A., Levine, X.J., 2010. Water vapor and the dynamics OF climate changes. Rev. Geophys. 48 https://doi.org/10.1029/2009RG000302.

Scoccimarro, E., Gualdi, S., Villarini, G., Vecchi, G.A., Zhao, M., Walsh, K., Navarra, A., 2014. Intense precipitation events associated with landfalling tropical cyclones in response to a warmer climate and increased CO2. J. Clim. 27, 4642–4654. https://doi.org/10.1175/JCLI-D-14-00065.1.

Shiogama, H., Hirata, R., Hasegawa, T., Fujimori, S., Ishizaki, N.N., Chatani, S., Watanabe, M., Mitchell, D., Lo, Y.T.E., 2020. Historical and future anthropogenic warming effects on droughts, fires and fire emissions of \chem{CO_{2}} and PM$_{2.5}$ in equatorial Asia when 2015-like El Niño events occur. Earth Syst. Dyn. 11, 435–445. https://doi.org/10.5194/esd-11-435-2020.

Sillmann, J., Kharin, V.V., Zwiers, F.W., Zhang, X., Bronaugh, D., 2013. Climate extremes indices in the CMIP5 multimodel ensemble: Part 2. Future climate projections. J. Geophys. Res. Atmos. 118, 2473–2493. https://doi.org/10.1002/jgrd.50188.

UNEP, 2019. The Emissions Gap. United Nations Environment Programme, Nairobi.

Van Oldenborgh, G.J., Van Der Wiel, K., Sebastian, A., Singh, R., Arrighi, J., Otto, F., Haustein, K., Li, S., Vecchi, G., Cullen, H., 2017. Attribution of extreme rainfall from hurricane harvey. Environ. Res. Lett. https://doi.org/10.1088/1748-9326/aa9ef2. August 2017.

Vial, J., Dufresne, J.-L., Bony, S., 2013. On the interpretation of inter-model spread in CMIP5 climate sensitivity estimates. Clim. Dynam. 41, 3339–3362. https://doi.org/10.1007/s00382-013-1725-9.

Walsh, K.J.E., Camargo, S.J., Vecchi, G.A., Daloz, A.S., Elsner, J., Emanuel, K., Horn, M., Lim, Y.-K., Roberts, M., Patricola, C., Scoccimarro, E., Sobel, A.H., Strazzo, S., Villarini, G., Wehner, M., Zhao, M., Kossin, J.P., La Row, T., Oouchi, K., Schubert, S., Wang, H., Bacmeister, J., Chang, P., Chauvin, F., Jablonowski, C., Kumar, A., Murakami, H., Ose, T., Reed, K.A., Saravanan, R., Yamada, Y., Zarzycki, C.M., Luigi Vidale, P., Jonas, J.A., Henderson, N., 2015. Hurricanes and climate: the U.S. Clivar working group on hurricanes. Bull. Am. Meteorol. Soc. 96 https://doi.org/10.1175/BAMS-D-13-00242.1.

Wang, S.Y.S., Zhao, L., Yoon, J.H., Klotzbach, P., Gillies, R.R., 2018. Quantitative attribution of climate effects on Hurricane Harvey's extreme rainfall in Texas. Environ. Res. Lett. https://doi.org/10.1088/1748-9326/aabb85.

Wehner, M.F., Reed, K., Fuyu, L., Prabhat Bacmeister, J., Chen, C.-T., Paciorek, C., Gleckler, P., Sperber, K., Collins, W.D., Andrew, G., Christiane, J., 2014. The effect of horizontal resolution on simulation quality in the Community Atmospheric Model, CAM5.1. J. Adv. Model. Earth Syst. 6, 980–997. https://doi.org/10.1002/2013MS000276.

Wehner, M., Prabhat Reed, K.A., Stone, D., Collins, W.D., Bacmeister, J., 2015. Resolution dependence of future tropical cyclone projections of CAM5.1 in the U.S. CLIVAR hurricane working group idealized configurations. J. Clim. 28, 3905–3925. https://doi.org/10.1175/JCLI-D-14-00311.1.

Wehner, M., Stone, D., Mitchell, D., Shiogama, H., Fischer, E., Graff, L.S., Kharin, V.V., Lierhammer, L., Sanderson, B., Krishnan, H., 2018. Changes in extremely hot days under stabilized 1.5 and 2.0\,{\degree}C global warming scenarios as simulated by the HAPPI multi-model ensemble. Earth Syst. Dyn. 9, 299–311. https://doi.org/10.5194/esd-9-299-2018.

Yang, B., Qian, Y., Lin, G., Leung, R., Zhang, Y., 2012. Some issues in uncertainty quantification and parameter tuning: a case study of convective parameterization scheme in the WRF regional climate model. Atmos. Chem. Phys. 12, 2409–2427. https://doi.org/10.5194/acp-12-2409-2012.

Zelinka, M.D., Myers, T.A., McCoy, D.T., Po-Chedley, S., Caldwell, P.M., Ceppi, P., Klein, S.A., Taylor, K.E., 2020. Causes of higher climate sensitivity in CMIP6 models. Geophys. Res. Lett. 47, e2019GL085782 https://doi.org/10.1029/2019GL085782.